J Nanopart Res (2020) 22: 7
https://doi.org/10.1007/s11051-019-4715-y

RESEARCH PAPER

Light absorption in visible–NIR range by linear copper clusters (n = 2–22) with monoatomic thickness: a TD-DFT study

Alexey V. Markin · Natalia E. Markina · Ammar J. Al-Alwani · Alexander A. Skaptsov

Received: 21 August 2019 / Accepted: 13 November 2019 / Published online: 2 January 2020

Abstract The authors theoretically investigated absorbance spectra of the hypothetical 1D Cu clusters with 2–22 atoms and monoatomic thickness. In contrast to 3D isomers with interband transitions only (< 600 nm; intrinsic for any copper nanostructure), the 1D clusters possess strong absorbance bands within 650–1800 nm range depending on the cluster size (NIR bands). The band location in NIR range was explained by low binding number per copper atom that leads to weaker coupling of 4*s* electrons within the conduction band and reducing energy gap between vacant and occupied orbitals. The NIR bands are formed by HOMO → LUMO transitions and their large intensity was explained by highly hybridized *sp* character of HOMO and LUMO and by the low contribution of 3*d* electrons (< 10%). The analysis of the number of electrons involved to the formation of NIR bands demonstrates their prominent plasmonic (collective) character. For example, the NIR band of the cluster with 20 atoms (1636 nm) is formed by excitation of 5 electrons. In contrast, 0.35 and 0.44 electrons were involved to the formation of all absorbance bands within visible–NIR range (400–1000 nm) for spherical and tetrahedral 3D isomers, respectively. The results are in qualitative agreement with experimental results for copper nanorods and nanowires which also possess strong bands in the red–NIR range (> 600 nm) compared to the nanoparticles with spherical geometry. Additionally, the large clusters (16–22 atoms) possess multiple bands in NIR range that is also in agreement with the experiment.

Keywords Copper nanoparticles · Plasmonic properties · Surface plasmon resonance · Interband transitions · Time-dependent density functional theory · Modeling and simulation

Introduction

One-dimensional (1D) metallic nanoparticles (nanorods and nanowires) possess prominent and tunable surface plasmon resonance (SPR) in NIR range of wavelengths (Sönnichsen et al. 2002; Khlebtsov and Khlebtsov 2007). This feature enables to generate SPR in the nanoparticles incorporated inside complex biological matrices minimizing or avoiding generation of side processes such as photodestruction and fluorescence of the matrix. As the results, such nanoparticles were proposed as the promising tool in photothermal anticancer therapy (Dykman and Khlebtsov 2012). Additionally, SPR bands of these nanoparticles are sensitive to the changes of dielectric constant of local environment that was used for development of various analytical systems (Cao et al. 2014).

Electronic supplementary material The online version of this article (https://doi.org/10.1007/s11051-019-4715-y) contains supplementary material, which is available to authorized users.

A. V. Markin (✉) · N. E. Markina · A. J. Al-Alwani · A. A. Skaptsov
Saratov State University, Astrakhanskaya 83, Saratov 410012, Russia
e-mail: av_markin@mail.ru

A. J. Al-Alwani
Babylon University, Babylon, Iraq

Although gold is the dominating material for fabrication of plasmonic nanostructures, copper has been also proposed as a promising alternative due to its cost-efficiency and availability. For example, copper nanostructures demonstrated competitive performance in surface-enhanced Raman spectroscopy (Markin et al. 2018). Despite the numerous reports regarding to 1D copper-based nanostructures (Bhanushali et al. 2015), there is a limited number of reports which demonstrate the structures with prominent SPR response in the NIR range (Zong et al. 2005; Duan et al. 2009; Oh et al. 2011). Zong et al. and Duan et al. studied dependence of SPR generation in copper nanorods and nanowires (CuNRs and CuNWs) on angle of incidence of the light field with respect to the long rod/wire axis. Duan et al. also showed that SPR bands in CuNWs depend on the length, thickness, and mean distance between adjacent wires. Oh et al. showed that a single CuNR can also possess multiple SPR bands in NIR range attributed to dipole and quadrupole modes.

To support experimental data, some of listed examples also contain the results of the simulations of plasmonic properties using the Mie–Gans approach (Zong et al. 2005) and discrete dipole approximation using the corresponding bulk dielectric functions (Oh et al. 2011). Unfortunately, these approaches do not enable to get information about electronic structure of the nanostructures in ground and excited states. On the other hand, electronic structure methods like time-dependent density functional theory (TD-DFT) can provide information about (i) allowed electronic transitions and (ii) electronic structure (i.e., chemical reactivity) of the nanostructures both in ground and excited states (Morton et al. 2011). This information can be of particular usefulness for explanation of photon/plasmon-assisted process taking place on the surface of copper-based nanostructures such as Raman enhancement through charge-transfer mechanism (Wu et al. 2008).

However, TD-DFT was mainly used for study of optical (plasmonic) properties of the Cu clusters (2–20 atoms) with low aspect ratio, i.e., spherical shaped structures (Baishya et al. 2011; Lecoultre et al. 2011; Anak et al. 2014). Additionally, the main attention in these studies was directed to the analysis of UV-visible part of the spectra. Lecoultre et al. used the calculation results to interpret experimental UV-visible spectra of Cu clusters incorporated to rare gas (neon) matrix. Baishya et al. compared calculated absorbance spectra of 3D Cu clusters with their theoretical results for Ag and Au clusters. Using zigzag Cu chains, the authors also demonstrated that the highly prolate or oblate Cu clusters possess tunable absorbance bands in NIR range of wavelengths which are in agreement with the results of the Mie–Gans approach. Gao et al. (2012) performed comparative study of 1D copper, silver, and gold clusters focusing on the influence of metal nature on the absorbance spectra. However, the authors did not address to the factors which cause differences between absorbance spectra of 1D and 3D Cu cluster.

The aim of current study is the further investigation of excited states of 1D Cu clusters with particular emphasis to the NIR range of wavelengths. The investigation includes analysis of influence of 3*d* electrons, cluster length (number of atoms), and interatomic distance on the excitations. The hypothetical Cu clusters with 2 to 22 atoms, linear geometry, and the maximal aspect ratio (monoatomic thickness) were chosen in order to facilitate interpretations by excluding other factors such as deviation of interatomic distance, angles, and binding number per atom.

Methods

TD-DTF calculations were carried out using the Firefly v.8.2 software (Granovsky n.d.; Schmidt et al. 1993). Los Alamos National Laboratory 2 double-ξ (LANL2DZ) basis set with pseudo-potential approach was chosen as widely used and resource-effective basis set for theoretical studies of the Cu clusters and their plasmonic properties (Wu et al. 2008; Gao et al. 2012). PBE0 hybrid functional was used due to its suitability for the accurate description of excited states (Adamo and Barone 1999; Jacquemin et al. 2011). The number of excited states in the computations was enough to calculate absorbance states with the energy up to ~ 3 eV (~ 400 nm). In order to minimize influence of partial linear dependence in the basis set, SCF density convergence threshold and the cutoff level for discarded integrals were fixed at 10^{-7} and 10^{-11}. DFT precision was also increased by increasing number of radial points per atom and order of Lebedev angular grid to 99 and 41, respectively. The convolution of the absorbance spectra (FWHM 0.1 eV) and the spectra of density of states (FWHM 0.3 eV) was performed using the GaussSum 3.0 software (O'Boyle et al. 2008). The Cu clusters with even number of the atoms and singlet multiplicity were used because the Firefly v. 8.2 enables

performing TD-DFT calculations only for closed-shell systems. The interatomic distance corresponded to the bulk copper, 2.556 Å (Kittel 1971), was used in the study. The ellipsoidal and tetrahedral isomers of the Cu cluster with 20 atoms and optimized geometry (LANL2DZ/PBE0; Table S1 in Online Resource) were used for comparison.

Results and discussions

Absorbance spectra

Calculated absorbance spectra of the Cu clusters in visible–NIR range are shown in Fig. 1. The spectra were calculated only for the cluster with even number of electrons because of software limitation to treat closed-shell electronic systems only. The possible optical susceptibility of the clusters with odd number of atoms is discussed in a separate section ("Light absorbance by the clusters with odd number of atoms"). Preliminary analysis of the electron contributions to the excited states showed that the excitations can be divided to (i) interband electron transitions and (ii) conduction band excitations. The interband transitions consist of multiple electron transitions from valence band (3*d* orbitals partially hybridized with *p* and *s* orbitals) to conduction band (vacant 4*sp* orbitals). These excitations require photons with more than 2 eV energy (< 600 nm; Fig. 1(a)) and are intrinsic for any copper-based nanostructure. The excitations in conduction band require photons with lower energy and correspond to the bands observed in red–NIR range of wavelengths (NIR bands; Fig. 1(b)). According to the studies of linear monoatomic sodium, potassium, and silver clusters (Yan et al. 2007; Yan and Gao 2008), the NIR bands occur due to oscillation of electron gas formed by *ns* electrons along the cluster (longitudinal excitations). Additionally, large Cu clusters (n = 16–22) possess the bands between interband and conduction band excitations (red bands; Fig. 1(c)). These bands can be assigned as the mixture between conduction band excitations of higher order and interband transitions.

Besides of longitudinal conduction band excitations, two transverse excitations (end and central resonances) were also reported for 1D metallic clusters (Yan and Gao 2008). However, the bands of these excitations were found in UV–blue range of wavelengths and experience blue shift with growth of the cluster length, e.g., for potassium clusters they were observed < 496 nm. Because these excitations require higher photon energy than longitudinal ones, they significantly overlap with intensive interband excitations ($(n-1)d \rightarrow nsp$) of the metals which are generally used for fabrication of plasmonic nanostructures (copper, silver, and gold). Therefore, we further analyze the interband and longitudinal conduction band excitations only because plasmonic properties of copper nanostructures in the visible–NIR range are the most interesting for analytical and biomedical applications.

Interband transitions

Influence of cluster size

Because the range of energy corresponded to 3*d* orbitals has high density of states (DOS) (− 8 to − 6.5 eV range in Fig. 2a), the interband excitations overlap each other significantly. Therefore, all absorbance bands with the energy above ~ 2 eV (< 600 nm) consist of several excited states (≥ 2); an example is shown in Fig. 2b (see also Table S2 for details). Consequently, the values of oscillator strength (OS) for the bands within 400–600 nm range were calculated by integrating OS values of the contributing excitations. The influence of the Cu cluster size on the band position and integrated OS is shown in Fig. 2c, d. The bands within 400–500 nm range (violet and blue bands; Fig. 2c, d) experience red shift and the growth of OS value with increase of the cluster size. We explain this behavior by significant decrease of the energy of vacant molecular orbitals (MOs) (LUMO + n, n = 0–4; Fig. 2a). The reduction of energy gap between occupied 3*d* and vacant 4*sp* MOs results in the decreasing of photon energy required for the excitation, i.e., to the red shift of the bands. For the growth of integrated OS values, we also explain by decrease of band gap. Although the number of 3*d* and 4*s* electrons grows equally with increase of the cluster size, the decrease of the energy gap leads to increase of the fraction of 3*d* electrons participated to the excitations due to the excitations from deeper MOs and 10-fold excess of 3*d* electrons in Cu atoms compared to 4*s* electrons.

The size dependence of the bands with the lower excitation energy (green and orange bands; Fig. 2c, d) is less systematic. The positions of the bands between 550–580 nm are not changed or experience blue shift and the OS values of these bands are generally

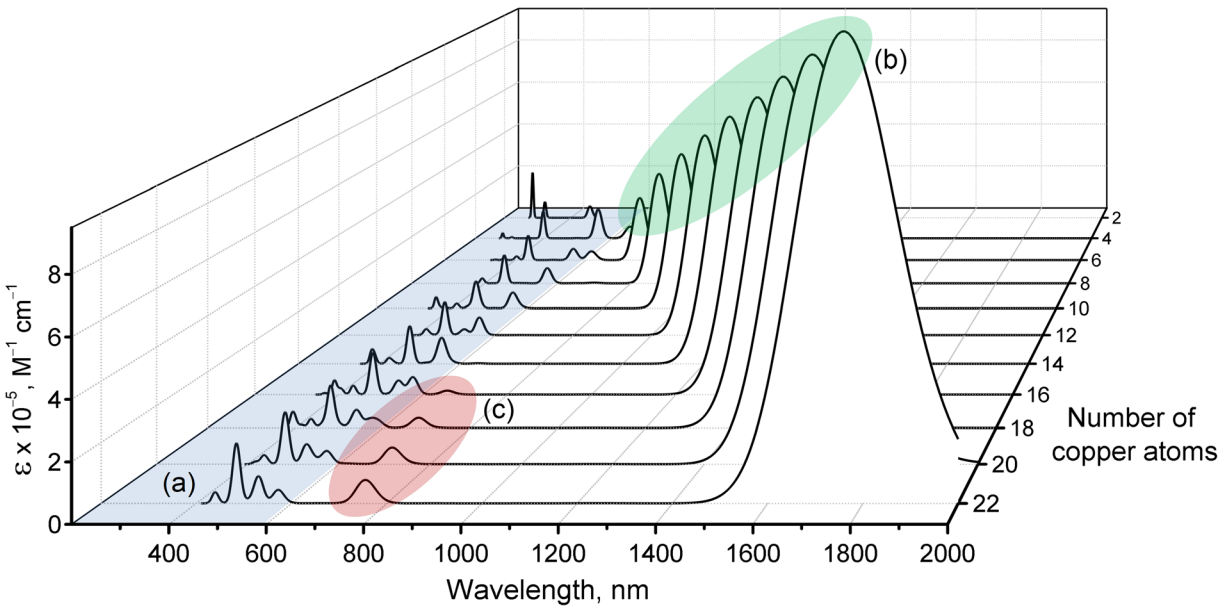

Fig. 1 Calculated absorbance spectra of linear one-atom-thick copper clusters. The bands (a) correspond to interband transitions and the sets of bands (b) and (c) correspond to valence band transitions. Absorbance is represented in the units of molar attenuation coefficient (ε)

decreased. On the other hand, the bands below 550 nm (for the clusters with 16–22 atoms) experience larger blue shift and their OS values grow. These results can be interpreted as the decrease of contribution of 4*s* electrons to the excitations that increases band energy. Additionally, the growth of contribution of 3*d* electrons leads to increase of the OS values as it is observed for the bands in 400–500 nm range. Baishya et al. (2011) also observed the increasing contribution of 3*d* electrons to the interband transitions with the growth of the Cu clusters with 3D geometry. The authors also explain this fact by the direct involving of 3*d* electrons to the low-energy excitations due to their hybridization with 4*s* energy levels and, additionally, by the screening of *s* electrons by *d* electrons (core polarization effect). Therefore, we can conclude that 1D and 3D Cu clusters have the similar dependence of the interband transitions on the cluster size.

Influence of the shape

The absorbance spectra the Cu clusters with 20 atoms and various geometries were compared to understand the influence of the shape on the excited states (Fig. 3). In order to minimize the influence of fixed interatomic distance in the case of the linear isomer, the absorbance spectrum was calculated using the cluster with the distance corresponding to the minimal total energy (0.2352 nm; Fig. S1).

The detailed analysis of excited states of the linear isomer shows that the optically susceptible MOs always have 5–15% and 2–5% contribution of *s* and *p* characters, respectively, depending on the MO energy (Fig. 4(a)). This fact is explained by forbidding direct transitions of 3*d* electrons to vacant MOs (4*sp*) in the case of optically allowed transitions. Thus, the excitations based on interband transitions can occur only from *d* orbitals hybridized with *s* and *p* orbitals (3*d*/3*p*, 3*d*/4*s*, and 3*d*/4*p*). It is remarkable that *p* and *d* components of the optically susceptible MOs are mainly oriented along the cluster. Therefore, the excitations based on interband transitions in the visible range are also oriented in the longitudinal direction.

The comparison of absorbance spectra shows that the linear Cu cluster possesses absorbance bands with larger OS values (Fig. 3). However, the formation of the multiple bonds per atom in the case of 3D isomers decreases the energy of 4*s* electrons and increases the number of the hybrid 3*d*(*s*,*p*) MOs and their hybridization degree (Fig. 4(b, c)). Thus, the probability of the interband transitions (absorbance) in the case of 3D clusters is expected to be much larger than that of the linear isomer. To explain this discrepancy, the analysis of DOS for all isomers was performed (Fig. 4(a'–c')). The results show

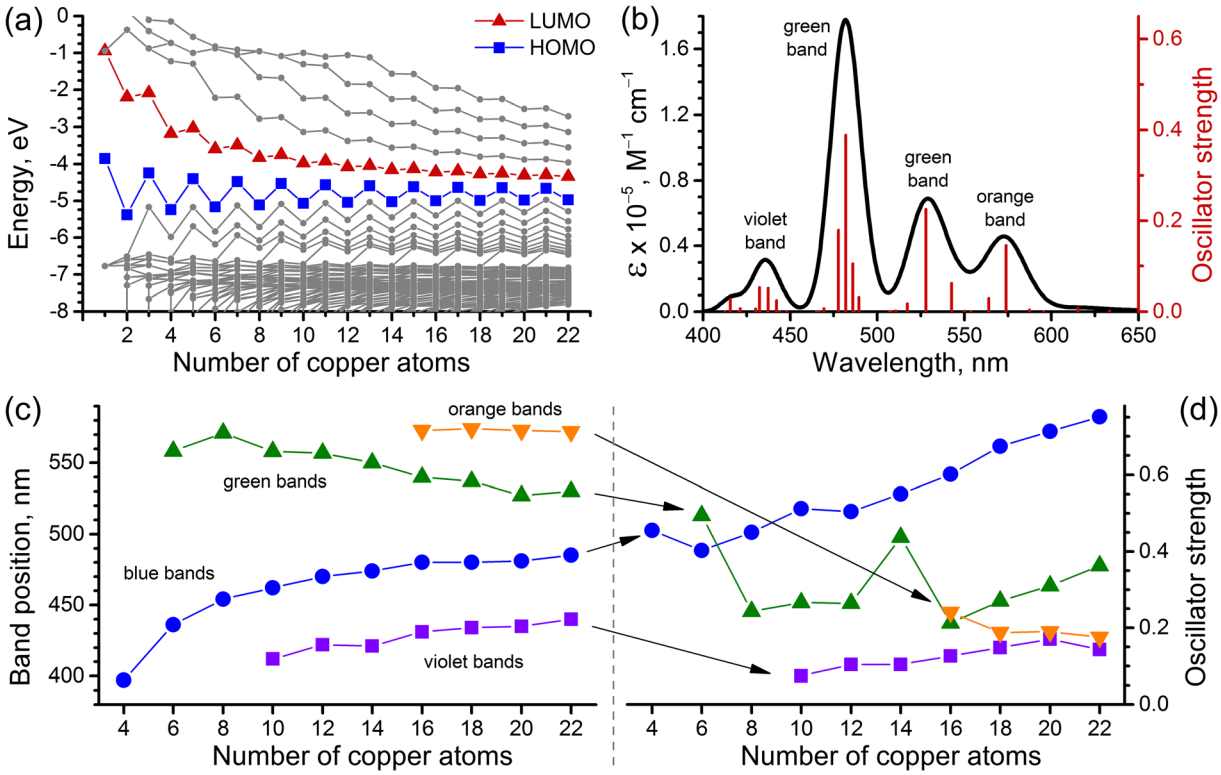

Fig. 2 The influence of the Cu cluster size on **a** the energy of the molecular orbitals which can be optically active within UV-visible–NIR range, **c** the position, and **d** integrated oscillator strength of the interband transition bands. **b** Absorbance spectrum of Cu cluster with 20 atoms in visible range and excited states participated to the spectrum formation

that the 3D isomers have larger separation between occupied and vacant MOs. Therefore, the strong absorbance for these clusters expected to be at higher excitation energies (< 400 nm) compared to the linear isomer.

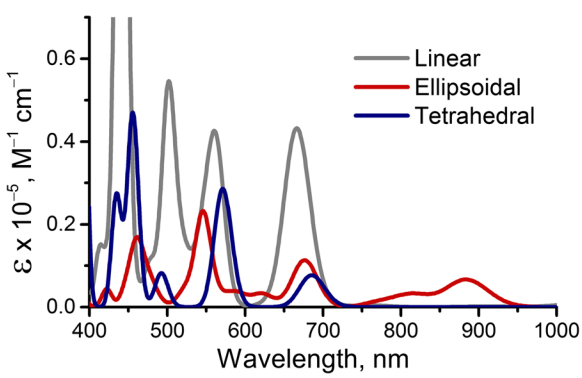

Fig. 3 Comparison of the calculated absorbance spectra of the linear Cu cluster with 20 atoms with the spectra of its 3D isomers; the images of the isomers are represented in Fig. 4(b', c')

Conduction band excitations

NIR bands

NIR bands are represented by the strong absorbance bands in the red–NIR range (650–1800 nm; Fig. 1(b)). In contrast to interband transitions, these bands have the linear dependence on the cluster size (Fig. 5a). The linear correlation between band OS value and the cluster size was previously demonstrated in theoretical results for alkaline metallic chains (Yan et al. 2007; Yan and Gao 2008). However, the linear correlation between band position and cluster size was not previously reported and we explain this linearity in terms of standing plasmon polariton waves (Schider et al. 2003).

Except of the clusters with 2 and 4 atoms, the NIR bands of other Cu clusters are mainly formed by the HOMO → LUMO transitions. The band of the cluster with two atoms has the 23% contribution of the interband transitions ($3d \rightarrow 4sp$). The band of the cluster with 4 atoms consists of HOMO − 2 → LUMO (53%) and HOMO → LUMO (45%) transitions both of which

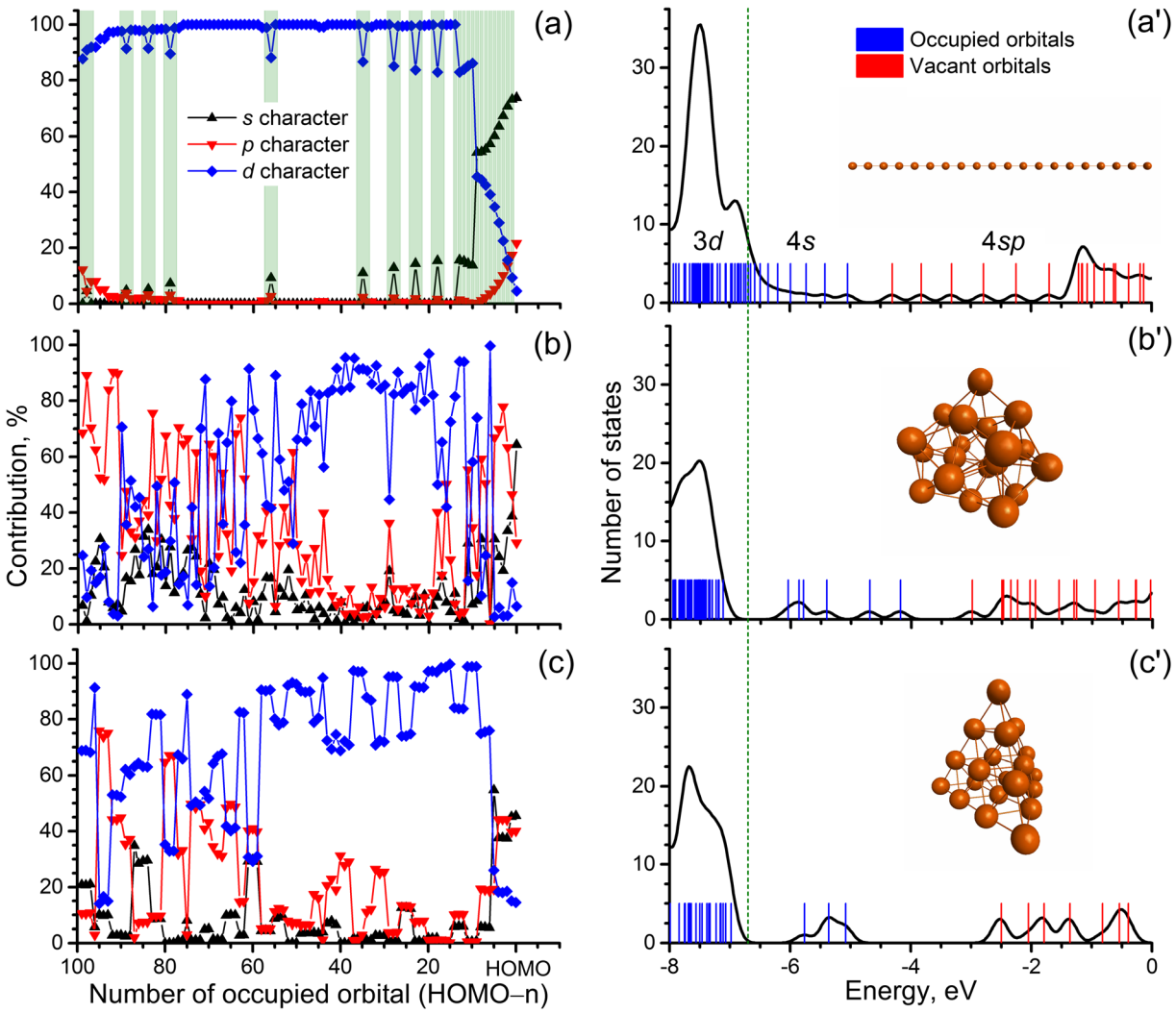

Fig. 4 The angular character of the occupied molecular orbitals (a–c) and density of states (a'–c') for the Cu clusters with 20 atoms and different shapes. Highlighted molecular orbitals in (a) correspond to optically susceptible orbitals

are belong conduction band. Thus, only the band of the cluster with 2 atoms was excluded from the analysis.

The analysis of DOS and the orbital angular momentum of the MOs (Fig. 4(a, a')) shows that 1D Cu clusters have the smallest gap between vacant and occupied MOs and their HOMO level possesses larger *s* character compared to one of 3D clusters. We explain this difference by lower binding number per copper atom in the case of 1D Cu clusters and, consequently, weaker coupling of 4*s* electrons within the conduction band. These facts explain the appearance of the absorbance bands in the NIR range and their large probability (intensity) compared to the bands of 3D Cu clusters.

The growth of the cluster size does not affect the contribution of 3*d* electrons to HOMO significantly (5–8%), while leading to the gradual growth of the *sp* hybridization degree (Fig. 5b). Because $s \rightarrow s$ and $p \rightarrow p$ orbital transitions of the electrons are forbidden, namely, the hybridized (*sp*) character of HOMO and LUMO and the low contribution of 3*d* electrons are responsible for high probability of the transitions, i.e., high absorbance.

The presence of strong absorbance bands in NIR range is in qualitative agreement with the experimental results observed by Oh et al. and Duan et al. for CuNRs and CuNWs (Oh et al. 2011; Duan et al. 2009). Thus, NIR bands can be assigned as analogues of longitudinal dipole modes in the real 1D Cu nanostructures. Unfortunately, the hypothetical character of the Cu clusters and the high length deviation of real CuNRs/

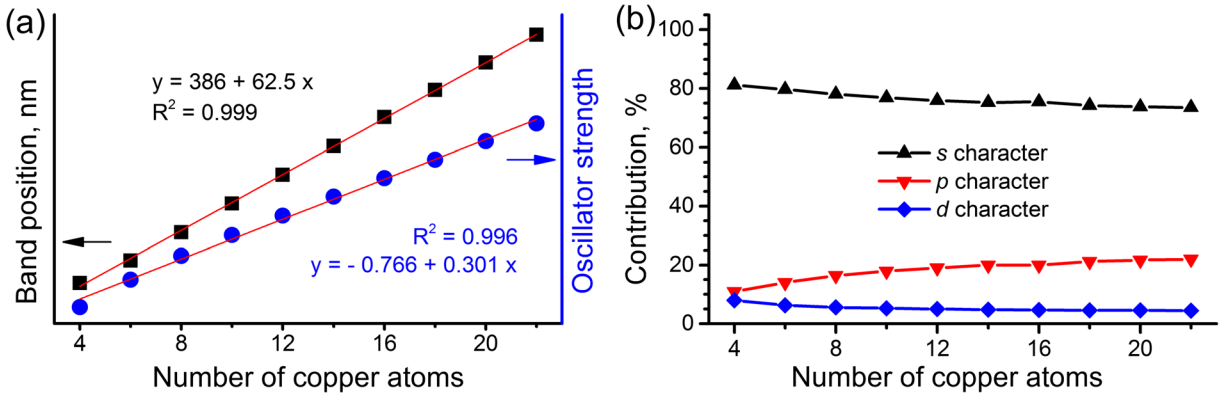

Fig. 5 Influence of the Cu cluster size on **a** position and oscillator strength of the conduction band excitations and **b** the orbital angular character of the highest occupied molecular orbital (HOMO)

CuNWs restrict precise quantitative comparison of the results. Additionally, the contribution of CuNRs with different length to the total absorbance spectrum can result in overlap between dipole and quadrupole resonances. However, there are some agreements with experimental results regarding small copper clusters.

Lecoultre et al. experimentally and theoretically investigated absorbance spectra of the 3D Cu clusters (1–9 atoms) in neon matrix (Lecoultre et al. 2011). The authors found that theoretical results for the cluster with 3 atoms have the remarkable difference with the experimental results due to presence of the band with relatively high intensity and unexpectedly low energy (2.46 eV/504 nm). The authors considered for calculations only clusters with optimized 3D geometry; however, the linear Cu cluster with 3 atoms can probably be also stable, contributing to the final absorbance spectrum. Using this hypothesis, we incorporated the results of Lecoultre et al. for this cluster to our results for the Cu clusters with the optimal interatomic distance (0.2352 nm; Fig. S1). Additionally, ~ 0.1–0.2 eV blue shift of the absorbance band caused by matrix effect (solid neon) (Kolb et al. 1984; Lecoultre et al. 2011) was also accounted. Despite the calculation error and interference with the spectrum of the triangular isomer, the satisfactory agreement was found for OS values (Fig. 6). However, the band position is significantly shifted from the main trend (48 nm/0.227 eV) that we mainly attribute to the open-shell electronic structure of this cluster (additionally discussed in the "Light absorbance by the clusters with odd number of atoms" section).

Red bands

These bands appear within the short range of wavelengths (600–800 nm) and only for large Cu clusters (16–22 atoms). The presence of several excitations within conduction bands is in agreement with multiple SPR bands in NIR range (dipole and quadrupole modes) which were observed in CuNRs and CuNWs by Oh et al. (2011). The comparable intensity of these bands and the bands of interband transitions as well as the significantly lower intensity compared to NIR bands (more than one order) are also in agreement with the experimental results of Oh et al. Therefore, these bands can be assigned as analogues of longitudinal quadrupole modes in CuNRs.

Because quadrupole bands are blue shifted and require larger photon energy, they can be influenced by interband transitions. The analysis of the MOs involved

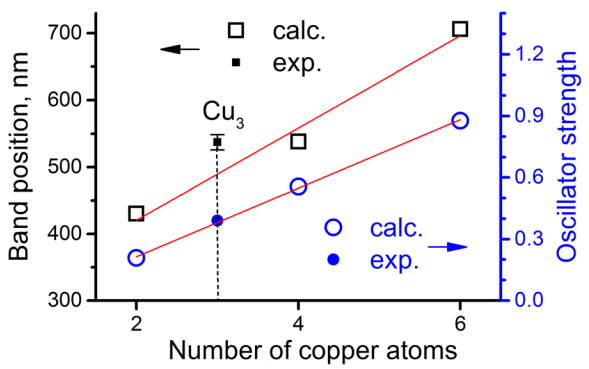

Fig. 6 The comparison of theoretical (2, 4, and 6 atoms) and experimental (3 atoms) results for the conduction band excitations in the linear Cu clusters. The theoretical results were obtained using the clusters with the optimized interatomic distance (0.2352 nm; Fig. S1)

to the excitations shows that red bands mainly consist of multiple transitions (generally 4–9) from HOMO − n to LUMO + n (where n = 1–3) with the contribution of electron transitions from inner lying (3d) occupied orbitals. This contribution is below 50% for the clusters with 18–22 atoms and ~ 80% for the cluster with 16 atoms. However, the linear dependence of the band position and OS value of red bands on the cluster size (Fig. S2) can indicate that, namely, the conduction band excitations determine the characteristics of these bands (as in the case of NIR bands).

Influence of interatomic distance

Above we explained the difference between absorbance spectra of 1D and 3D Cu clusters by larger number of chemical bonds between copper atoms that leads to larger coupling of s electrons and increasing their energy. In order to additionally study this effect, we studied an influence of the interatomic distance on the conduction band excitations (Fig. S3).

As it was expected, the reduction of interatomic distance leads to the blue shift of the bands and reduction of their OS values. For the NIR bands, we also found that the OS value of the smallest cluster (16 atoms) possesses the larger sensitivity to distance changes compared to other clusters (Fig. S3a). This fact can be explained by stronger influence of interband transitions as a result of larger overlap with 3d orbitals. The detailed analysis of the interatomic distance influence on the NIR bands was performed for the Cu cluster with 20 atoms only (Fig. S3b). The band position demonstrates the larger response on the change of interatomic distance compared to OS value. For example, the band of the Cu cluster with the optimal interatomic distance is 8.6% shifted relative to the cluster with the distance corresponded to the bulk copper, but the OS value is reduced to 3.4% only. We explain this result by small dependence of the orbital angular character in the interatomic distance (Fig. S4a); the maximal changes are around 5% decrease of s character and ~ 15% increase of d and p characters (at the optimal interatomic distance; Fig. S4b). Thus, we can conclude that the influence of the cluster shape on the excited states and resulting absorbance spectra (Fig. 3) is drastically larger compared to influence of the interatomic distance, particularly in the case of OS values.

Light absorbance by the clusters with odd number of atoms

The possible optical susceptibility of the clusters with open-shell electronic structure was estimated by analyzing energies and angular moments of MOs (Figs. 2a and S5). The dependence of the MO energies on the cluster size for the open-shell clusters is similar to that of closed-shell ones, i.e., the MO energies reach almost constant values with the growth of the clusters (Fig. 2a). However, the total dependencies of MO energies and band gap values on the cluster size have oscillating character (Figs. 2a and S5a) because the energy of conduction band MOs is increased in the case of clusters with open-shell structure. For example, the comparison of the clusters with 20 and 19 atoms shows that the last one has 2–7% (0.11–0.33 eV) and 1–7% (0.06–0.21 eV) larger energy values for HOMO − n (n = 0–9) and LUMO + n (n = 0–4), respectively, while the difference for inner lying MOs was found below 0.5% (< 0.02 eV) (Fig. S5b). The analysis of orbital angular moments does not show significant differences between the clusters with open and closed shells (Fig. S5c). Therefore, we expect that the band positions of the conduction band excitations (NIR and red band) will experience the largest influence of open-shell character of the electronic structure and lead to red shift of the bands. In contrast, the OS values (intensity of absorbance) are expected to be independent of this factor.

The made conclusions are in qualitative agreement with experimental results for 3D Cu clusters with open-shell electronic structure. According to the results for neutral Cu clusters (2–9 atoms) embedded to a solid neon matrix (Lecoultre et al. 2011), the clusters with odd numbers of atoms always possess absorbance bands in the range of 2.0–2.5 eV, while the closed-shell clusters absorb the light below 2.5 eV only. Therefore, the significant red shift (0.226 eV) of the experimental band observed for the Cu cluster with 3 atoms is in agreement with discussed conclusions as well as independence of OS value on the open-shell electronic state (Fig. 6).

Plasmonic character of the bands

Because SPR implies collective oscillation of the electron cloud, we performed differentiation of the plasmonic properties for the interband transitions and conduction band excitations using the Thomas–Reiche–Kuhn sum rule. The rule states that the sum of OS over all

transitions participated to the formation of a particular band equals to the number of electrons involved to the formation of this band. The analysis of integrated OS for the Cu cluster with 20 atoms showed that only 1.4 electrons are involved to the all interband excitations (400–600 nm range). Even lower values were found for the optical transitions within the visible–NIR range (> 400 nm) for 3D Cu clusters: 0.35 and 0.44 electrons for spherical and tetrahedral clusters, respectively. The value of similar order (~ 0.2 electrons) was obtained for the red bands (600–800 nm range). On the other hand, the single NIR band (1636 nm for the cluster with 20 atoms) is formed by excitation of around 5.2 electrons (Fig. 5a). Thus, the absorbance bands below 600 nm (i.e., all interband transitions) can be hardly assigned as plasmonic (collective electron oscillations) implying intra-atomic electron transitions only. Although the experimental results regarding to optical properties of 1D Cu chains with monoatomic thickness are not available yet, our conclusions are in the qualitative agreement with the experimental results for CuNRs (Oh et al. 2011) as well as prolate copper nanoparticles (Pastoriza-Santos et al. 2009) and copper nanoshells (Wang et al. 2005). The authors of these reports also observed significantly larger extinction in the red–NIR range (> 600 nm) compared to interband transitions.

Conclusions

Therefore, accounting qualitative (for nanoparticles) and semi-quantitative (3-atom clusters) agreement of our theoretical results with the experimental results from literature, we can conclude that the linear 1D Cu clusters with monoatomic thickness are an appropriate model for simulation of the tunable plasmon resonances during quantum chemical studies. Additionally, the hypothetical character of the model enables facilitates interpretation of the results by fixing multiple factors which appear during the study of 3D clusters (e.g., deviation of interatomic distance, angles, binding number per atom). These features make the model particularly attractive for high-precision theoretical studies of the various photon/plasmon-assisted chemical processes, e.g., Raman enhancement through charge-transfer mechanism and photocatalysis.

Funding information The work was supported by RFBR according to the research project № 17-03-00537.

Compliance with ethical standards

Conflict of interest The authors declare that they have no conflict of interest.

References

Adamo C, Barone V (1999) Toward reliable density functional methods without adjustable parameters: the PBE0 model. J Chem Phys 110:6158–6170

Anak B, Bencharif M, Rabilloud F (2014) Time-dependent density functional study of UV-visible absorption spectra of small noble metal clusters (Cun, Agn, Aun, n = 2–9, 20). RSC Adv 4:13001–13011

Baishya K, Idrobo JC, Ogut S, Yang M, Jackson KA, Jellinek J (2011) First-principles absorption spectra of Cun (n = 2–20) clusters. Phys Rev B 83:245402

Bhanushali B, Ghosh P, Ganesh A, Cheng W (2015) 1D Copper nanostructures: progress, challenges and opportunities. Small 11:1232–1252

Cao J, Sun T, Grattan KTV (2014) Gold nanorod-based localized surface plasmon resonance biosensors: a review. Sensors Actuators B Chem 195:332–351

Duan JL, Cornelius TW, Liu J, Karim S, Yao HJ, Picht O, Rauber M, Muller S, Neumann R (2009) Surface plasmon resonances of Cu nanowire arrays. J Phys Chem C 113:13583–13587

Dykman L, Khlebtsov N (2012) Gold nanoparticles in biomedical applications: recent advances and perspectives. Chem Soc Rev 41:2256–2282

Gao B, Ruud K, Luo Y (2012) Plasmon resonances in linear noble-metal chains. J Chem Phys 137:194307

Granovsky A (n.d.) A. Firefly Version 8. http://classic.chem.msu.su/gran/firefly/index.html. Accessed 05 August 2019

Jacquemin D, Mennucci B, Adamo C (2011) Excited-state calculations with TD-DFT: from benchmarks to simulations in complex environments. Phys Chem Chem Phys 13:16987–16998

Khlebtsov BN, Khlebtsov NG (2007) Multipole plasmons in metal nanorods: scaling properties and dependence on particle size, shape, orientation, and dielectric environment. J Phys Chem C 111:11516–11527

Kittel C (1971) Introduction to solid-state physics. Wiley, New York

Kolb DM, Rotermund HH, Schrittenlacher W, Schroeder W (1984) Optical spectrum of matrix-isolated Cu2. J Chem Phys 80:695–700

Lecoultre S, Rydlo A, Félix C, Buttet J, Gilb S, Harbich W (2011) Optical absorption of small copper clusters in neon: Cun, (n = 1–9). J Chem Phys 134:074303

Markin AV, Markina NE, Popp J, Cialla-May D (2018) Copper nanostructures for chemical analysis using surface-enhanced Raman spectroscopy. Trends Anal Chem 108:247–259

Morton SM, Silverstein DW, Jensen L (2011) Theoretical studies of plasmonics using electronic structure methods. Chem Rev 111:3962–3994

O'Boyle NM, Tenderholt AL, Langner KM (2008) Cclib: a library for package-independent computational chemistry algorithms. J Comput Chem 29:839–845

Oh MK, Baik HJ, Kim SK, Park S (2011) Multiple surface plasmon resonances in silver and copper nanorods. J Mater Chem 21:19069

Pastoriza-Santos I, Sánchez-Iglesias A, Rodríguez-González B, Liz-Marzán LM (2009) Aerobic synthesis of Cu nanoplates with intense plasmon resonances. Small 5:440–443

Schider G, Krenn JR, Hohenau A, Ditlbacher H, Leitner A, Aussenegg FR, Schaich WL, Puscasu I, Monacelli B, Boreman G (2003) Plasmon dispersion relation of Au and Ag nanowires. Phys Rev B 68:155427

Schmidt MW, Baldridge KK, Boatz JA, Elbert ST, Gordon MS, Jensen JH, Koseki S, Matsunaga N, Nguyen KA, Su S, Windus TL, Dupuis M, Montgomery JA (1993) General atomic and molecular electronic structure system. J Comput Chem 14:1347–1363

Sönnichsen C, Franzl T, Wilk T, von Plessen G, Feldmann J, Wilson O, Mulvaney P (2002) Drastic reduction of plasmon damping in gold nanorods. Phys Rev Lett 88:077402

Wang H, Tam F, Grady NK, Halas NJ (2005) Cu nanoshells: effects of interband transitions on the nanoparticle plasmon resonance. J Phys Chem B 109:18218–18222

Wu DY, Liu XM, Duan S, Xu X, Ren B, Lin SH, Tian ZQ (2008) Chemical enhancement effects in SERS spectra: a quantum chemical study of pyridine interacting with copper, silver, gold and platinum metals. J Phys Chem C 112:4195–4204

Yan J, Gao S (2008) Plasmon resonances in linear atomic chains: free-electron behaviour and anisotropic screening of d electrons. Phys Rev B 78:235413

Yan J, Yuan Z, Gao S (2007) End and central plasmon resonances in linear atomic chains. Phys Rev Lett 98:216602

Zong RL, Zhou J, Li B, Fu M, Shi SK, Li LT (2005) Optical properties of transparent copper nanorod and nanowire arrays embedded in anodic alumina oxide. J Chem Phys 123: 094710

Terms and Conditions

Springer Nature journal content, brought to you courtesy of Springer Nature Customer Service Center GmbH (“Springer Nature”).
Springer Nature supports a reasonable amount of sharing of research papers by authors, subscribers and authorised users (“Users”), for small-scale personal, non-commercial use provided that all copyright, trade and service marks and other proprietary notices are maintained. By accessing, sharing, receiving or otherwise using the Springer Nature journal content you agree to these terms of use (“Terms”). For these purposes, Springer Nature considers academic use (by researchers and students) to be non-commercial.
These Terms are supplementary and will apply in addition to any applicable website terms and conditions, a relevant site licence or a personal subscription. These Terms will prevail over any conflict or ambiguity with regards to the relevant terms, a site licence or a personal subscription (to the extent of the conflict or ambiguity only). For Creative Commons-licensed articles, the terms of the Creative Commons license used will apply.
We collect and use personal data to provide access to the Springer Nature journal content. We may also use these personal data internally within ResearchGate and Springer Nature and as agreed share it, in an anonymised way, for purposes of tracking, analysis and reporting. We will not otherwise disclose your personal data outside the ResearchGate or the Springer Nature group of companies unless we have your permission as detailed in the Privacy Policy.
While Users may use the Springer Nature journal content for small scale, personal non-commercial use, it is important to note that Users may not:

1. use such content for the purpose of providing other users with access on a regular or large scale basis or as a means to circumvent access control;
2. use such content where to do so would be considered a criminal or statutory offence in any jurisdiction, or gives rise to civil liability, or is otherwise unlawful;
3. falsely or misleadingly imply or suggest endorsement, approval , sponsorship, or association unless explicitly agreed to by Springer Nature in writing;
4. use bots or other automated methods to access the content or redirect messages
5. override any security feature or exclusionary protocol; or
6. share the content in order to create substitute for Springer Nature products or services or a systematic database of Springer Nature journal content.

In line with the restriction against commercial use, Springer Nature does not permit the creation of a product or service that creates revenue, royalties, rent or income from our content or its inclusion as part of a paid for service or for other commercial gain. Springer Nature journal content cannot be used for inter-library loans and librarians may not upload Springer Nature journal content on a large scale into their, or any other, institutional repository.
These terms of use are reviewed regularly and may be amended at any time. Springer Nature is not obligated to publish any information or content on this website and may remove it or features or functionality at our sole discretion, at any time with or without notice. Springer Nature may revoke this licence to you at any time and remove access to any copies of the Springer Nature journal content which have been saved.
To the fullest extent permitted by law, Springer Nature makes no warranties, representations or guarantees to Users, either express or implied with respect to the Springer nature journal content and all parties disclaim and waive any implied warranties or warranties imposed by law, including merchantability or fitness for any particular purpose.
Please note that these rights do not automatically extend to content, data or other material published by Springer Nature that may be licensed from third parties.
If you would like to use or distribute our Springer Nature journal content to a wider audience or on a regular basis or in any other manner not expressly permitted by these Terms, please contact Springer Nature at

onlineservice@springernature.com